

# NJC

New Journal of Chemistry

Accepted Manuscript

A journal for new directions in chemistry

This article can be cited before page numbers have been issued, to do this please use: E. B. Aydin, M. Aydin and M. K. Sezgintürk, *New J. Chem.*, 2020, DOI: 10.1039/D0NJ03183F.



This is an Accepted Manuscript, which has been through the Royal Society of Chemistry peer review process and has been accepted for publication.

Accepted Manuscripts are published online shortly after acceptance, before technical editing, formatting and proof reading. Using this free service, authors can make their results available to the community, in citable form, before we publish the edited article. We will replace this Accepted Manuscript with the edited and formatted Advance Article as soon as it is available.

You can find more information about Accepted Manuscripts in the [Information for Authors](#).

Please note that technical editing may introduce minor changes to the text and/or graphics, which may alter content. The journal's standard [Terms & Conditions](#) and the [Ethical guidelines](#) still apply. In no event shall the Royal Society of Chemistry be held responsible for any errors or omissions in this Accepted Manuscript or any consequences arising from the use of any information it contains.

# Development of an ultra-sensitive electrochemical immunosensor using PPy-NHS functionalized disposable ITO sheet for detection of interleukin 6 in real human serums

Received 00th January 20xx,  
Accepted 00th January 20xx

Elif Burcu Aydın<sup>a\*</sup>, Muhammet Aydın<sup>a</sup>, Mustafa Kemal Sezgintürk<sup>b</sup>

DOI: 10.1039/x0xx00000x  
[www.rsc.org/](http://www.rsc.org/)

A label-free impedimetric immunosensor based on conjugated poly(pyrrole N-hydroxy succinimide) (PPyr-NHS) polymer covered disposable indium tin oxide electrode (ITO) was fabricated for ultrasensitive determination of interleukin 6 (IL 6) antigen. In this sensing platform, PPy-NHS polymer, which carried a number of succinimide groups on its end side, was used as a matrix material for the first time. This synthesized polymer had excellent biocompatibility and good electrical conductivity. In addition, the utilization of this material as a matrix material provided direct immobilization of IL 6 receptor (IL6R), which was employed as a biorecognition element. The preparation of working electrode, the successful attachment of IL 6R and specific interaction between IL6R and IL 6 antigen were confirmed by electrochemical impedance spectroscopy (EIS) and cyclic voltammetry (CV) techniques. Moreover, the working electrode surface was characterized by Scanning electron microscopy (SEM), Atomic force microscopy (AFM), Fourier transform infrared spectroscopy (FTIR) and Raman spectroscopy during its construction. Impedimetric method was employed for quantification of IL 6 antigen. Under optimizing experimental conditions, the designed sensing platform could detect IL 6 antigen with a wide detection range from 0.03 pg/mL to 22.5 pg/mL with a relatively low detection limit of 10.2 fg/mL. In addition, the developed biosensor had outstanding sensitivity and specificity, good repeatability and reproducibility, high stability and reusability. Additionally, the designed sensing tool was successfully used in human serum samples. Consequently, the suggested immunosensor was clinically useful in the early detection of the prostate cancer by direct determination of the serum IL 6 antigen level after simple dilution.

## Introduction

Cancer is one of the leading causes of death<sup>1</sup>, with prostate cancer being one of the most common type in man globally and its early detection is the key to the high potential, easy, low-cost and effective therapy<sup>2</sup>. Several potential biomarkers such as protein biomarkers, circulating tumor cells, circulating tumor DNA and cell fragments are found in blood and utilized for disease diagnosis<sup>3,4</sup>. The usage of cancer biomarkers in disease diagnosis provides early detection of cancer and increases the survival rate of patients<sup>5</sup>. To date, several methods such as enzyme-linked Immunoassay (ELISA), radioimmunoassay and fluorescence immunoassay methods have been reported for cancer biomarkers detection. The traditional ELISA is one of the most preferred method for quantification of biomarkers in biological fluids based on spectrophotometric reading. This method offers reproducible, sensitive, specific and reliable results that makes it a suitable tool in scientific research and clinical diagnosis. Besides these advantages, it has some disadvantages such as time-consuming and tedious procedure, the short shelf life of the labeled antibody, excess reagent consumption, high cost and the narrow detection range<sup>6</sup>. Additionally, the detection limit of classic ELISA method is barely less than the nanomolar concentration level, which is insufficient to obtain the clinical threshold of many protein biomarkers, which are important in the early stage of diseases<sup>7</sup>. Furthermore, the ELISA method cannot be reused for many measurements and its regeneration is not possible<sup>8</sup>. Taking into account all of these disadvantages, electrochemical strategies have gained interest owing to their intrinsic properties such as simple

operation, rapid response, low-cost and compatibility with miniaturation technology<sup>9-11</sup>.

Interleukin 6 (IL 6) is a pro-inflammatory cytokine, which has a significant role in immunity. It stimulates growth and differentiation of B cells, secretion of immunoglobulins, differentiation and activation of T cells and macrophages<sup>12</sup>. In addition, it acts as an anti-inflammatory myokine in the inflammatory process<sup>13</sup>. IL 6 is a circulating protein, which is present in healthy human plasma around 6 pg/mL. The overexpression of IL 6 is a sign of tumor genesis, tumor growth, and cancer cell differentiation<sup>14</sup>. The high concentrations of IL 6 biomarker are related to the prostate cancer<sup>15</sup>. Until now different analytical methods including bioassays, immunoassays, molecular biology techniques and flow cytometry have been used for IL 6 detection<sup>12, 15, 16</sup>. Among them, enzyme-linked immunosorbent assay (ELISA) is the most common method. The sensitivity of ELISA is high, but it suffers from some interferences. Because of this, new approaches, which can increase the sensitivity and selectivity of the analytical techniques should be found to detect some biomarkers found at ultra-low levels in the earlier diagnosis of prostate cancer<sup>17</sup>. Different studies for IL 6 biomarker detection have been reported in literature. Wang et al. (2010) constructed an amperometric immunosensor based on polydopamine-gold nanoparticles (AuNPs) modified glassy carbon electrode (GCE), in which the linear detection range and detection limit were found as 4-800 pg/mL and 10 pg/mL, respectively<sup>18</sup>. Liu et al. (2013) manufactured an electrochemiluminescence biosensor based on graphene oxide/polyaniline nanowires/CdSe quantum dots nanocomposite modified GCE, and the detection limit of this biosensing system was found as 0.17 pg/mL<sup>17</sup>. A sensitive aptasensor was fabricated by Tertis et al. (2019) by using p-aminobenzoic acid, p-aminothiophenol and AuNPs modified GCE. A thiol-terminated aptamer, which was specific to IL 6 antigen was utilized as biorecognition element and the immunosensor displayed

<sup>a</sup> Namik Kemal University, Scientific and Technological Research Center, Tekirdağ-TURKEY. E-mail: ebbahadir@nku.edu.tr; Tel: +90 282 250 1137

<sup>b</sup> Çanakkale Onsekiz Mart University, Faculty of Engineering, Bioengineering Department, Çanakkale-TURKEY

high sensitivity, wide linear detection range (5 pg/mL-100 ng/mL) and ultra-low detection limit (1.6 pg/mL)<sup>19</sup>.

Indium tin oxide (ITO) is a conductive transparent oxide material and ITO film coated substrates have been utilized as an electrode platform for biosensors. The advantages of ITO substrate as working electrode are high stability, ease of combination with electrode fabrication process and lower cost than gold and platinum electrodes<sup>20</sup>. Immobilization of biorecognition molecules on the working electrode is a crucial step in the designing of biosensors<sup>21</sup>. The physical and chemical features of the matrix materials utilized in the fabrication of the biosensors have an important effect on their sensitivity and stability<sup>22</sup>. In order to increase the detection performances of biosensors for determination of cancer biomarkers, more and more electrochemical biosensors have been developed and fabricated<sup>23-25</sup>. In recent years, conjugated polymers are introduced to modify the electrode surface due to their excellent physical and chemical features<sup>26,27</sup>. They can transfer the electron produced during the biochemical reaction and they are suitable matrices for biorecognition element immobilization<sup>28</sup>. Poly(thiophene), poly(pyrrole) and poly(aniline) are traditional conjugated polymers and up to now different conducting polymers have been synthesized and utilized in the biosensor development<sup>29-32</sup>. Poly(pyrrole) is extensively studied matrix material because of its advantages in biosensors development. Electrical conductivity, easy functionalization, biocompatibility and stability make this material an excellent component for electrochemical biosensor fabrication<sup>34</sup>. In this study, *PPyr-NHS* polymer was synthesized and polymerized for the first time to use as a suitable matrix for biorecognition molecule immobilization and the developed immunosensor was successfully applied to cancer biomarker monitoring in human sera. This polymer had not only succinimide groups to anchor IL6R through amide bond, but also it exhibited good conductivity. In addition, the usage of *PPyr-NHS* polymer as a biosensor matrix material provided a biocompatible surface for IL6R and did not require the NHS/EDC activation step and IL6R covalently bound to polymer modified ITO surface.

## Experimental

### Chemicals and material

Unless otherwise noted, materials and solvents were obtained from commercial suppliers and used without further purification. 1-pyrrolopropionitrile (Pyr-CN), potassium bromide (KBr), potassium hydroxide (KOH), 4-dimethylamino pyridine (DMAP), anhydrous iron(III) chloride (FeCl<sub>3</sub>), N-Hydroxysuccinimide (NHS), 1-ethyl-3-(dimethyl-aminopropyl) carbodiimide hydrochloride (EDC), nitromethane (CH<sub>3</sub>NO<sub>2</sub>), chloroform (CHCl<sub>3</sub>), tetrahydrofuran (THF), hydrochloric acid (HCl), dimethylsulfoxide (DMSO), acetone, sulfuric acid (H<sub>2</sub>SO<sub>4</sub>), potassium chloride (KCl), potassium dihydrogen phosphate (KH<sub>2</sub>PO<sub>4</sub>), dipotassium phosphate (K<sub>2</sub>HPO<sub>4</sub>), potassium ferrocyanide (K<sub>4</sub>[Fe(CN)<sub>6</sub>]) and potassium ferricyanide (K<sub>3</sub>[Fe(CN)<sub>6</sub>]) were from Sigma-Aldrich (USA). ITO coated polyethylene terephthalate film (0.5 cm x 2 cm), human IL6R, human IL 6 antigen and bovine serum albumin (BSA) were purchased from Sigma-Aldrich (USA). IL 6R, IL 6 antigen and BSA solutions were prepared by a pH 7.4 phosphate buffer solution (PBS, 50 mM containing 1 M KCl). Interleukin 1α (IL 1α), p53 antigen (p53), neuron specific enolase (NSE) and tumor necrosis factor α (TNF α) were selected as interferences and they were purchased from Sigma-Aldrich (USA). The national guideline stated in the National regulations on clinical trials published on the issue of government gazette (Number: 28030, August 19, 2011) was followed. Moreover, the experiments

performed in this research was approved by the ethical committee of non-invasive clinical researches of Tekirdağ Namık Kemal University (Ethic committee approval number 2013/86/07/05).

### Apparatus and measurements

Fourier transform infrared (FTIR) spectrum was collected Bruker Company Vertex 70 spectrometer. Raman spectrum was recorded with a Thermo Company DXR Raman spectrometer (780-nm excitation laser). Proton Nuclear Magnetic Resonance spectra was carried out via Bruker Avance II (400 MHz) using CDCl<sub>3</sub> deuterated solvents. Electrochemical measurements (EIS and CV) were conducted on a Gamry workstation with a conventional three electrode system composed of a platinum wire as a counter, Ag/AgCl as a reference and an ITO sheet as a working electrode, respectively. EIS analyses were performed in [Fe(CN)<sub>6</sub>]<sup>3-/4-</sup> solution within the frequency range from 0.5 Hz to 50 kHz. CV analyses were performed in [Fe(CN)<sub>6</sub>]<sup>3-/4-</sup> solution at the range of -0.5 V - +1 V at a scan rate of 100 mVs<sup>-1</sup>. Electrochemical impedance measurements were performed by applying an alternating potential of 5 mV to the working electrode. The formal potential applied in the impedance studies was 0 V. Scanning electron microscope (SEM) images and energy dispersive X-ray (SEM-EDX) analysis were taken using Field Emission Scanning Electron Microscope QUANTA FEG-250. Atomic force microscopy (AFM) images were performed on an ambient AFM Nano-Magnetic Instrument in dynamic AFM mode. The scan rate was 5 μm/s with a resolution of 256 pixels per line. Three-dimensional (3D) AFM images were prepared via Nano-Magnetics image analyzer software.

### Synthesis of Monomer and polymer

#### Synthesis of acid-substituted Pyrrole Monomer (*Pyr-Pac*)

The starting monomer for the present synthesis was the known compound N-pyrrolylpropanoic acid (*Pyr-Pac*), which was prepared from 1-pyrrolopropionitrile. The synthesis was performed using a modified version of the protocol of Khan et al. (2007)<sup>33</sup> for the conversion of the nitrile group in 1-pyrrolopropionitrile. In short, 2.5 g (2.08 mmol) of 1-pyrrolopropionitrile was mixed with 15 mL potassium hydroxide solution (5 g, 8.9 mmol) and they were heated and stirred at 100°C under a reflux of dry nitrogen for overnight. The obtained product was acidified to pH 4 with 8 M HCl and it was extracted six times with diethyl ether. At the end of this process, the organic phase was dried over anhydrous MgSO<sub>4</sub> and solvent was evaporated. Thus, pure product was produced as a beige crystalline. (Yield: %87, 2.01g). FTIR (cm<sup>-1</sup>): 3500-3100; 2940-2884; 1695(carbonyl); 1600-1450; 1216; 931; 787, 724; 647; 613; 500(Fig. SI-2B). Raman (λ<sub>laser</sub>=780 nm): 1710 (C=O); 1570; 1462; 1322; 1145;1167; 932; 780; 695; 653; 620(Fig. SI-3A). <sup>1</sup>H-NMR (δH, ppm): 11.6 (Ha, 1H); 2.8 (Hb, 1H); 4.2 (Hc, 2H); 6.7 (Hd, 2H) and 6.2 (He, 2H) (Fig. SI-4).

#### Synthesis of succinimide substituted Pyrrole Monomer (*Pyr-NHS*)

Adapting a literature procedure, we used the Steglich esterification of *Pyr-Pac* with N-Hydroxysuccinimide.<sup>34,35</sup> Briefly, *Pyr-Pac* (0.7 g, 5 mmol), DMAP (0.056 g, 0.5 mmol), EDC (1.917 g, 10 mmol) and NHS (0.69 g, 6 mmol) were solved in dry tetrahydrofuran and were stirred at room temperature under argon flow for 48 hours. After that, reaction solvent was evaporated, and the organic layer in diethyl ether was washed repeatedly with ultrapure water. Finally, the product was dried over anhydrous magnesium sulfate and concentrated in rotary evaporation. (Yield:1.32g, 56%). FTIR (cm<sup>-1</sup>): 2940-2926 (CH); 1810, 1776, 1732(C=O); 1201; 1060; 890; 807; 717;

641 (Fig. SI-2C). Raman ( $\lambda_{\text{laser}}=780$  nm): 1816, 1779 (C=O); 1286; 1090; 995; 898; 815; 730; 665 (Fig. SI-3B).  $^1\text{H-NMR}$  ( $\delta\text{H}$ , ppm): 6.17 ppm (Ha, 2H), 6.70 ppm (Hb, 2H), 4.31 ppm (Hc, 2H), 3.08 ppm (Hd, 2H) ve 2.85 ppm (He, 4H) (Fig. SI-5).

### Synthesis of *N*-Succinimidyl Ester Polypyrrole (*PPyr-NHS*)

The succinimide functional group substituted polymer (*PPyr-NHS*) was prepared by using the previously reported oxidative polymerization method with minor adaptation<sup>36</sup>. The monomer *Pyr-NHS* (0.236 g, 1 mmol) was solved in chloroform (10 mL) in a two-necked round bottom flask and it placed in an ice-salt bath and a solution of 0.65 g (4 mmol) of anhydrous iron chloride ( $\text{FeCl}_3$ ) in 3 mL of nitro methane was added dropwise over 20 min. After stirring for 100 min at room temperature under argon gas, the black color reaction mixture was concentrated and precipitated in cold methanol. Then, dark brown precipitate was obtained by filtration and it was rinsed with ultrapure water and methanol. Finally, *PPyr-NHS* was dried using vacuum oven. (Yield: 0.32g, 45%). FTIR ( $\text{cm}^{-1}$ ): 2958, 2933(C-H); 1813, 1781, 1733 (C=O); 1421; 1362; 1201; 1065; 997; 807; 646 (Fig. SI-2D). Raman ( $\lambda_{\text{laser}}=780$  nm): 1815, 1780 (C=O); 1576; 1330; 1130; 1019; 990; 825 668 (Fig. SI-3C).

### Construction of the biosensing platform

Prior to use, the bare ITO electrode was successively rinsed in an ultrasonic cleaner with ethanol, soap solution and ultrapure water, and dried under an argon flow. Then, 10  $\mu\text{L}$  of synthesized *PPyr-NHS* polymer (0.24 mg/mL) was dropped on the ITO electrode and a thin film was formed on the ITO electrode by using a spin coater. Subsequently, the biorecognition element IL 6 Receptor was accomplished by dipping *PPyr-NHS* modified ITO substrate into 100  $\mu\text{L}$  PBS containing IL 6 Receptor (3 ng/mL) for 1 hour. After covalent attachment, the modified ITO electrode was incubated in BSA (0.5%) solution to block the free succinimide groups. Then, the ITO electrode was rinsed with ultrapure water to remove unattached

BSA molecules. In conclusion, the prepared ITO electrode was ready to measure of IL 6 antigen. After every step above mentioned, the modified electrodes were characterized by using EIS and CV methods. The whole fabrication process is illustrated in Scheme 1.

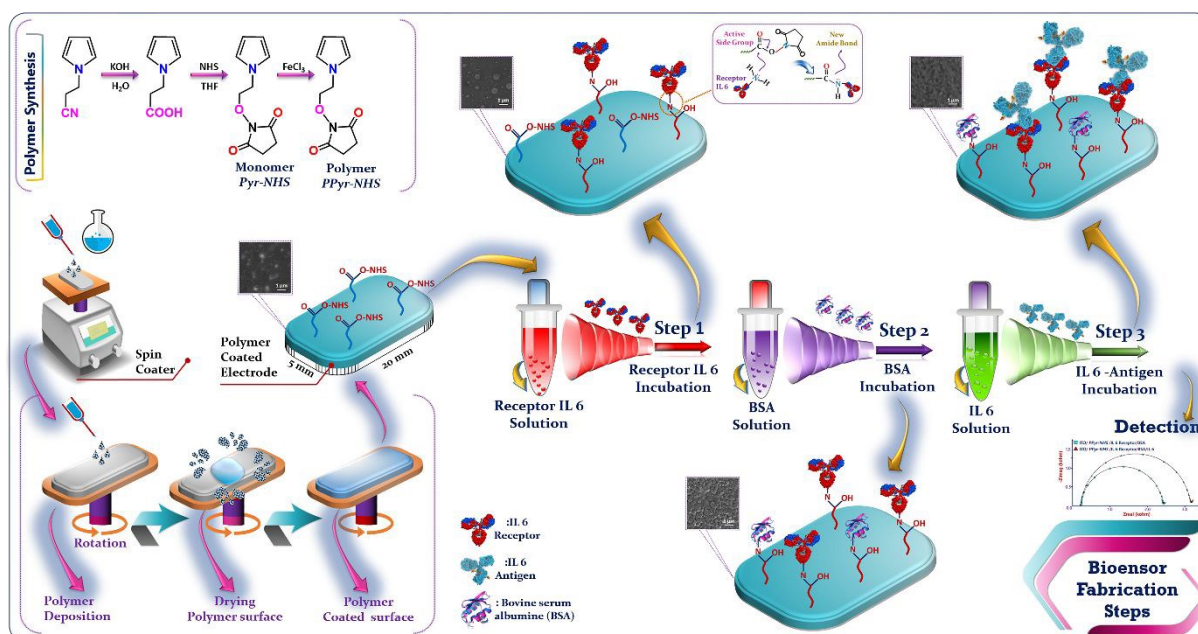
### Practical applicability of the IL 6 biosensor

The constructed biosensor was utilized for determination of IL 6 in order to verify its practical applicability. The IL 6 antigen level in the human sera was measured by the designed immunosensor, and standard addition method was used to examine the accuracy of the immunosensor.

### Results and Discussion

In this work, *PPyr-NHS* polymer modified IL 6 immunosensor was constructed by simple 3 preparation steps. The construction strategy of the label-free IL 6 immunosensor is depicted in Scheme 1. Since *PPyr-NHS* polymer had free succinimide groups, it was easily used to immobilize the IL6R biomolecules (Step 1). The free succinimide groups were blocked by BSA (Step 2) and lastly, the biorecognition event formation between IL6R and IL 6 antigen (Step 3).

For the synthesis of succinimide functional group substituted poly(pyrrole) polymer, we needed a series of reactions which were performed in three steps. The synthetic route of the *PPyr-NHS* polymer is illustrated in Scheme 1. The first step was the conversion reaction of nitrile group to acid group. In the second step, the steglich esterification of *N*-pyrrolylpropanoic acid with *N*-hydroxysuccinimide was utilized. In the final step, the succinimide substituted pyrrole monomer (*Pyr-NHS*) was polymerized via chemical oxidative coupling technique with anhydrous ferric chloride. The chemical structures of monomer and polymer were investigated by several spectral methods (FTIR and  $^1\text{H}$  NMR and Raman spectroscopy) to indicate the success of the synthesis method and results were illustrated in detail in the Supp. Inf. file.



**Scheme 1.** Schematic illustration of the composite preparation procedure and the fabrication process of the immunosensor.

### Chemical characterization of *PPyr-NHS* polymer coated ITO electrode and IL 6R attached ITO electrode

The FTIR spectra of *PPyr-NHS* polymer (A) and IL6R modified ITO electrode (B) are illustrated in Fig 1. As shown in Fig. 1A, the FT-IR spectra for polymer modified electrode showed two strong bands at  $1814\text{ cm}^{-1}$  and  $1782\text{ cm}^{-1}$  that proved characteristic carbonyl groups of the NHS ester<sup>37,38</sup>. The strong peak at  $1730\text{ cm}^{-1}$  was the evidence of the typical C=O stretching vibration of carbonyl groups<sup>39</sup>. When two FTIR spectra were analyzed, in the FTIR spectra of the Fig 1B, the disappearance of characteristic carbonyl bands of the NHS ester and new absorption bands at  $1652\text{ cm}^{-1}$  (amid I) and  $1551\text{ cm}^{-1}$  (amid II) proved the covalent bond formation of between succinimide groups of polymer and amino group of receptor (Scheme 1). The presence of polymer on the electrode surface and chemical interactions between polymer succinimide groups and amino groups of receptors were also examined with Raman spectroscopy.

Raman spectroscopy can give knowledge about the specific interactions in polymer blends, nucleic acids and large molecules. The one of the biggest advantages of Raman spectroscopy is the ease of sample preparation. Moreover, the relative intensity variation and the shift of Raman band proved the chemical interaction between polymer and receptors. The Raman spectra of *PPyr-NHS* modified electrode before IL6R immobilization (red line) and after IL6R immobilization (purple line) are displayed in Fig. 1C and 1D, respectively. The Raman spectra in Fig. 1C demonstrated that stretching vibrations of carbonyl bonds in succinimide groups were monitored at  $1815\text{ cm}^{-1}$  and  $1770\text{ cm}^{-1}$ . Amide I, amide II and amide III bond bands of protein structure are usually monitored mostly between  $1650\text{--}1680\text{ cm}^{-1}$ ,  $1480\text{--}1570\text{ cm}^{-1}$  and  $1235\text{--}1300\text{ cm}^{-1}$ , respectively<sup>41</sup>. The peaks of  $1656$ ,  $1530$  and  $1329\text{ cm}^{-1}$  were attributed characteristic peaks in IL 6R attached electrode surface.

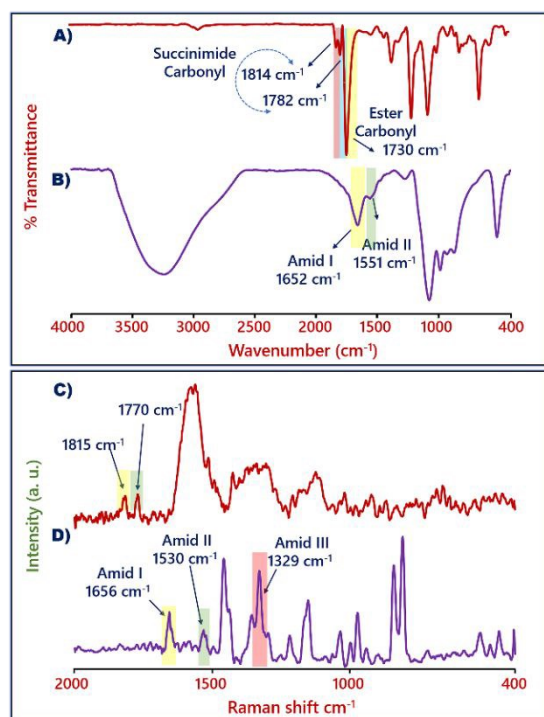


**Fig. 1.** FTIR measurements of *PPyr-NHS* coated ITO electrode (A) and IL 6R attached ITO electrode (B), Raman measurements of *PPyr-NHS* coated ITO electrode (C) and IL 6R attached ITO electrode (D).

### Electrochemical characterization of the immunosensing surface

EIS was utilized to characterize the fabrication process as it was one of the most powerful tools to investigate the interfacial property of the electrode surface. The impedance analysis results were fitted to an equivalent circuit (inset 1E), which was composed of the electrolyte solution resistance ( $R_s$ ), the surface electron transfer resistance ( $R_{ct}$ ), the Warburg impedance ( $Z_w$ ) and the constant phase element (CPE)<sup>42-44</sup>. Fig. 2A and 2B show the EIS and CV obtained in ferri/ferrocyanide solution (5 mM) containing 1M KCl at different electrode surface. The *PPyr-NHS* modified ITO electrode had a low  $R_{ct}$  because of the conductive property of *PPyr-NHS* polymer. Compared to polymer modified ITO electrode, the IL 6R immobilized ITO electrode displayed increased  $R_{ct}$  because of the successful immobilization of IL 6R. The IL 6R immobilization reduced the conductivity of the ITO surface and obstructed the electron transfer. Surface blocking with BSA led to a further increment in  $R_{ct}$  due to the insulativity of BSA protein. The specific biointeraction between IL6R and IL 6 antigen caused a protein layer coating that prevented the electron transfer. Moreover, the immunosensor was characterized by CV measurements, which provided valuable information about the variation formed on the modified electrode surface. The polymer coated ITO surface had high peak currents with enhanced electron transfer. After IL6R attachment onto the ITO surface, the peak currents decreased significantly due to non-conductivity of protein molecules. The BSA blockage step caused a hindrance effect to electron transfer because of non-conductive property of BSA molecules. When ITO surface was dipped in IL 6 antigen solution, the redox peak currents of ferri-ferro were decreased due to capturing of target IL 6 antigen by IL 6R. The results were well consistent with EIS responses, confirming the successful preparation of the immunosensor.

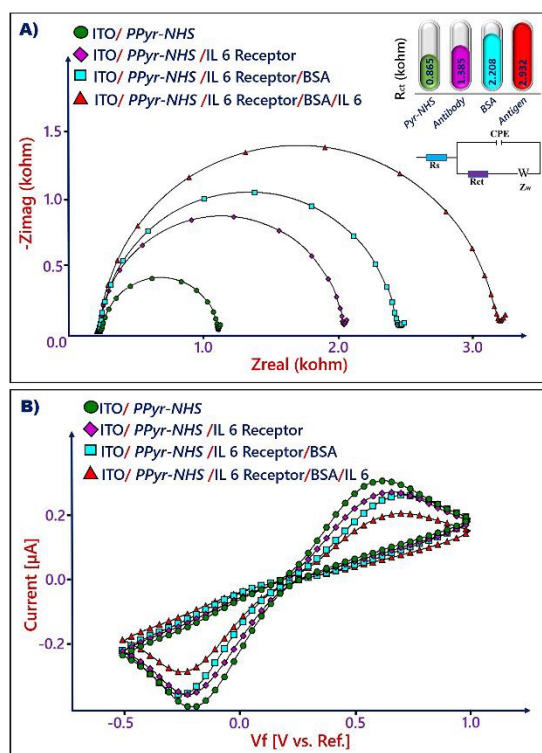


**Fig. 2.** Impedance (A) and voltammetric (B) characterization of the build-up process of proposed immunosensor. (Inset: Equivalent electrical circuit)

#### SEM and AFM characterizations of modified electrode surfaces

The surface topography of the IL 6 immunosensor for each construction stage was examined by SEM and AFM. Fig. 3A and 3B show SEM-EDX images of bare ITO substrate and PPyr-NHS polymer modified ITO substrate. EDX images were taken simultaneously with the SEM shown in Fig. 3C. The spectrum of bare ITO electrode shows the peaks that indium, tin, oxygen and carbon elements (Fig. 3A). After spin coating of polymer on the ITO substrate surface, the spectrum shows carbon, nitrogen, oxygen, indium, tin peaks. The peak of "N" element belongs to polymer, which has successfully coated on the bare ITO substrate surface (Fig. 3B). As illustrated in Fig. 3C, PPyr-NHS polymer was uniformly covered on the ITO substrate and the average roughness ( $R_a$ ) was measured as 17.8 nm over  $5 \times 5 \mu\text{m}^2$  area (Fig. 3D). After attachment of IL 6R on the polymer modified electrode, the SEM and AFM images illustrated that round-shaped macromolecules were immobilized on the electrode surface (Fig. 3E). The capturing of IL 6R molecules caused an increase in  $R_a$  value and it was measured as 48.1 nm over  $5 \times 5 \mu\text{m}^2$  area (Fig. 3F). The changes on the ITO surface illustrated that the modification of the electrode surface was obtained through the covalent binding. After BSA blockage step, a smooth surface was observed on the ITO surface (Fig. 3G). The  $R_a$  value was measured 20.5 nm over  $5 \times 5 \mu\text{m}^2$  area (Fig. 3H).

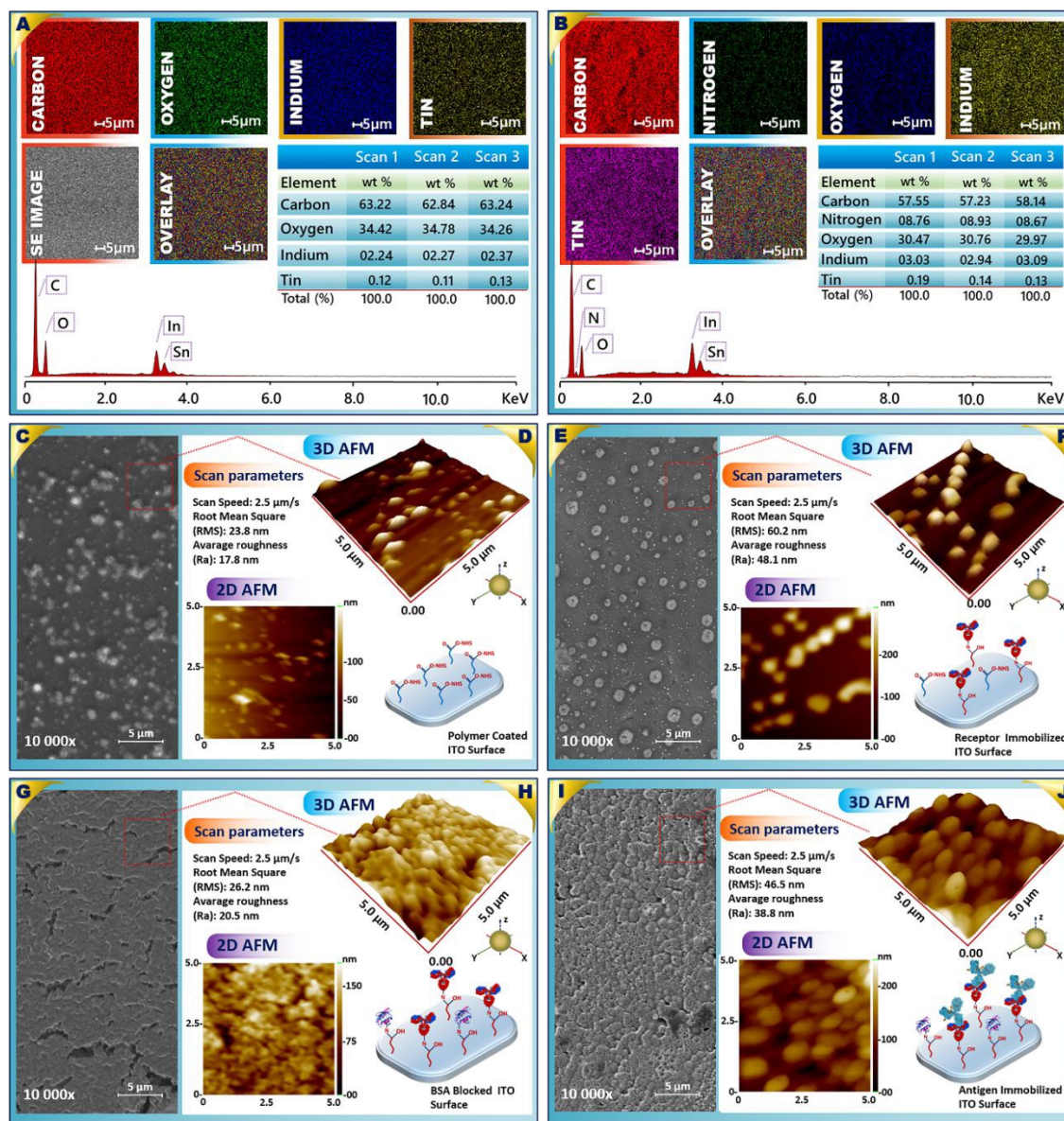


Fig. 3. SEM and AFM micrographs of the immunosensor construction stages.

The specific interaction between IL 6R and IL 6 antigen changed the electrode surface morphology and a protein layer was coated on the ITO surface (Fig. 3I). After this interaction, the  $R_a$  was measured as 38.8 nm over  $5 \times 5 \mu\text{m}^2$  (Fig. 3J). In conclusion, it was concluded that there was a perfect correlation between the results obtained with electrochemical and morphological techniques.

### Optimization of experimental conditions

To achieve optimal biosensing performance, polymer concentration, biorecognition element concentration and incubation period, and target antigen incubation period are key parameters.

The optimization of polymer concentration was conducted to obtain excellent biosensor response. The amount of polymer

coated on the ITO electrode could affect the analytical performance of the immunosensor and therefore, it was controlled by using different concentrations of polymer during immunosensor fabrication. Three different *PPyr-NHS* polymer concentrations (0.12 mg/mL, 0.24 mg/mL and 0.36 mg/mL) were tried, and the obtained biosensor signals were illustrated in Fig. 4A. The low polymer concentration led to low immunosensor response and caused a decrease in detection efficiency. Higher polymer concentration increased the immunosensor signal and 0.24 mg/mL was chosen as an optimum polymer concentration. The concentration of biorecognition elements is another important parameter. The usage of low receptor concentration caused a low immunosensor response and the high receptor concentration increased the cost of the biosensor. As displayed in Fig. 4B, the impedimetric signal was increased correspondingly

1  
2  
3  
4  
5  
6  
7  
8  
9  
10  
11  
12  
13  
14  
15  
16  
17  
18  
19  
20  
21  
22  
23  
24  
25  
26  
27  
28  
29  
30  
31  
32  
33  
34  
35  
36  
37  
38  
39  
40  
41  
42  
43  
44  
45  
46  
47  
48  
49  
50  
51  
52  
53  
54  
55  
56  
57  
58  
59  
60

with increasing with IL 6R concentration up to 15 ng/mL. The responses of immunosensors were similar when the IL 6R concentrations were 3 ng/mL and 15 ng/mL. Therefore, 3 ng/mL IL 6R level was selected for the next experiments (Fig. 4B). The IL 6R incubation time was another considerable parameter affected the immunosensor response. It could be seen that 45 min was enough for IL 6R incubation and 45-min incubation in IL 6R solution provided maximum immunosensor response. Because of

this, 45 min was utilized for the next experiments (Fig. 4C). Lastly, the antigen incubation time was optimized. As seen in Fig. 4D, the impedimetric response increased continuously with the incubation time. The impedimetric responses were similar after 45 min and 60 min incubation in IL 6 antigen solution and 45 min was adequate for IL 6 antigen incubation to form specific immunocomplex. Thus, 45 min was selected as the suitable incubating period and it was adopted in the following work.

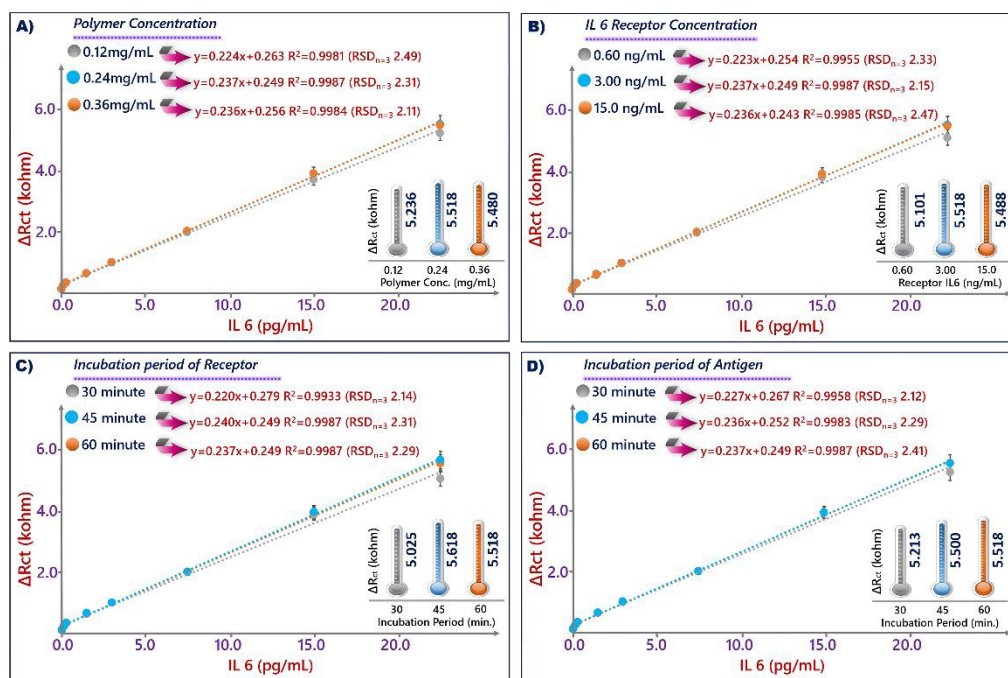


Fig. 4. The obtained EIS response after optimization experiments.

#### Analytical performance of the designed IL 6 immunosensor

Under optimum conditions, the analytical performance of the developed immunosensor was analyzed by varying IL 6 antigen concentrations. As illustrated in Fig. 5A, the impedimetric response increased with the increase of IL 6 antigen levels, indicating that the increasing amount of IL 6 antigens were specifically immobilized on the ITO surface and produced remarkable electrochemical signals. In addition, the increase of IL 6 antigen concentration led to decrease in peak currents because of non-conductive protein layer formation (Fig. 5B). The impedance analysis results were fitted to a Randles equivalent circuit. The changes in the  $R_{ct}$  of electrodes that incubated in different concentration of IL6 were calculated by the following equation;

$$R_{ct} = R_{ct}(\text{IL 6}) - R_{ct}(\text{BSA})$$

$R_{ct}(\text{IL6})$  and  $R_{ct}(\text{BSA})$  values corresponded to  $R_{ct}$  values after interaction between IL6R and IL6 antigen, and after BSA immobilization of ITO electrode, respectively. The impedimetric signals of the suggested immunosensor were linearly proportional to the IL 6 antigen level within the concentration range from 0.03 pg/mL to 22.5 pg/mL (Fig. 5C). The regression equation was

$\Delta R_{ct}(\text{kohm}) = 0.235 [\text{IL 6}] + 0.246$  ( $R^2 = 0.999$ ) with a limit of detection of 10.2 fg/mL at a signal to noise ratio of 3 (the standard deviation of the blank solution,  $n=5$ ). The quantification limit and sensitivity of the immunosensor were calculated as 34.1 fg/mL and  $1 \text{ pg mL}^{-1} \text{ kohm cm}^{-2}$ , respectively. The analytical characteristics of the designed immunosensor was also compared with some previous detection strategies and the results are given in table 1A. Apparently, the developed polymer based immunosensor had a low detection limit owing to conductive property of *PPy-NHS* polymer. Furthermore, the polymer synthesis procedure and immunosensor fabrication process were easier than other biosensors.

Single frequency impedance (SFI) is an analytical tool, which measures kinetic interaction between antibody and antigen at a fixed frequency. The fixed frequency is selected from Bode plot (Fig. SI- 6). In this study, 31 Hz frequency was utilized for SFI experiment. Therefore, the change in impedance during the specific immunoreaction was followed at 31 Hz as a function of time and phase angle in an electrochemical cell containing IL 6 antigen solution. As observed in Fig. 5D, the impedance was increased due to specific immunoreaction between receptor and antigen.

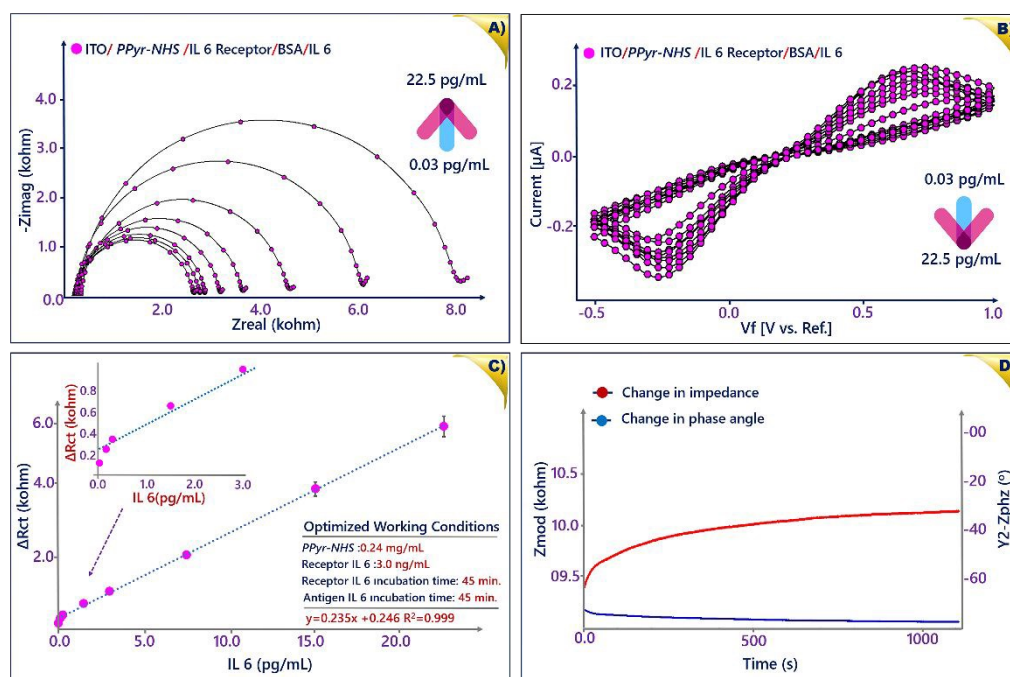


Fig. 5. (A and B) EIS and CV responses of the immunosensor at different IL 6 concentrations (0.03, 0.15, 0.3, 1.5, 3, 7.5, 15, 22.5 pg/mL), (C) calibration curve obtained after EIS measurements, (D) Single frequency impedance result.

**Repeatability, reproducibility, selectivity, regeneration and stability of the immunosensor**

In order to investigate the repeatability of the biosensing system, 20 different modified ITO electrodes were used to measure the IL 6 antigen at the same concentration (3 pg/mL). The relative standard deviation (RSD) was calculated as 3.2%, indicating acceptable repeatability of the immunosensor (Fig. 6A). Furthermore, the reproducibility of the biosensor was also examined. 10 different immunosensors were prepared at the same conditions and they were used for IL 6 antigen measurement. The RSD was calculated as 1.03%, indicating the good reproducibility (Fig. 6B).

Another important property of a good immunosensor is high selectivity<sup>45</sup>. The selectivity of the designed immunosensor was based on the recognition of IL 6 antigen by IL 6R. To examine the selectivity of the proposed immunosensor, a comparison study was performed by using interferent biomarkers. One of the IL 6R immobilized ITO electrode was incubated in PBS solutions containing interferent biomarkers (IL 1 $\alpha$ , TNF  $\alpha$ , p53 and NSE antigens with 300 pg/mL concentration), another IL 6R immobilized ITO electrode was incubated in PBS solutions containing interferent biomarkers (300 pg/mL) and IL 6 antigens (3 pg/mL). As expected, the impedimetric response of the target IL 6 antigen captured ITO electrode was higher than the impedimetric response of interferent biomarkers, which illustrated the higher selectivity of the developed immunosensor.

Besides, the regeneration of the immunosensor was also significant in practical analyses. The biosensing interface could be easily regenerated by immersion the ITO electrode into acidic solution (HCl, 10 mM) at room temperature for 5 min, followed by being rinsed with ultrapure water. After 8 regeneration steps, 75.96% of the initial signal was observed (Fig. 6C).

In addition, the developed immunosensor had an excellent storage stability. After long-term storage (4 °C in dry form) of the immunosensor, as much as 80.91% (eight weeks) of initial impedimetric response was preserved, displayed the suggested immunosensor could be utilized for IL 6 antigen determination with acceptable stability (Fig. 6D).

**Practical application of the IL 6 immunosensor in human sera**

To evaluate the applicability of the designed immunosensor, human sera were analyzed after 10-fold dilution by using the proposed immunosensor. To test accuracy of the immunosensor, standard addition method was utilized, and IL 6 antigens were added in diluted human sera. The analysis results are given in table 1B. It could be seen that the recoveries were between 100.17% and 100.99, which illustrated that the suggested electrochemical immunosensor had promising successful in real human sera analyses.

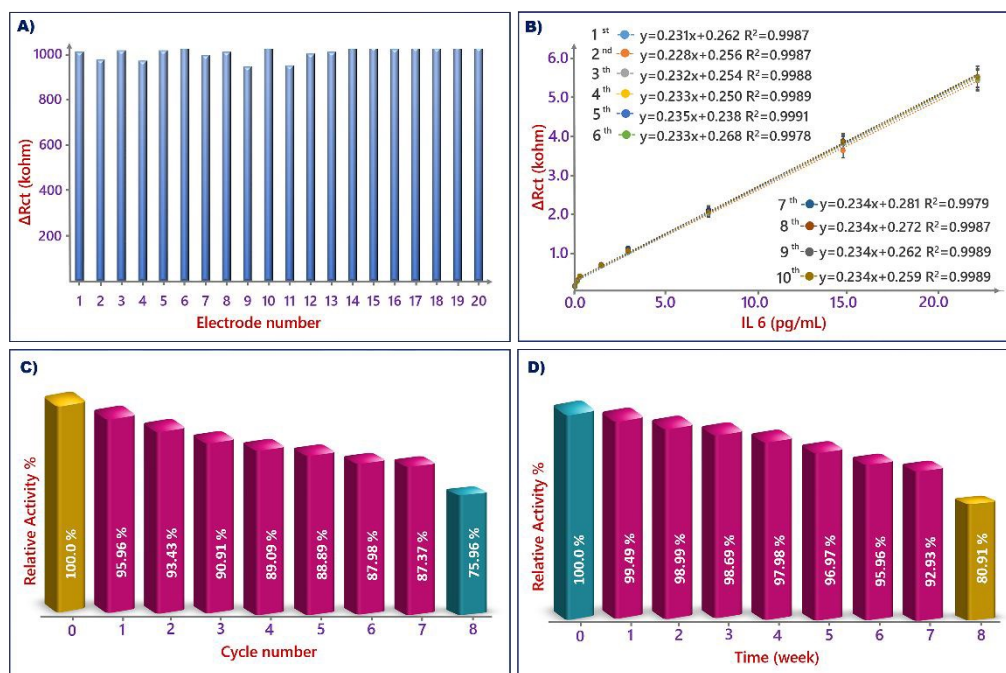


Fig. 6. Results of repeatability (A), Reproducibility (B), Regeneration (C) and Storage stability (D).

Table 1. Comparison with other works using different techniques for IL 6 detection (A), human sera results of the immunosensor.

(A) Modification	Electrode Type	Linear Range (pg/mL)	Detection limit (pg/mL)	Ref.
AuNPs/single walled carbon nanotubes (SWCNTs)	Si/SiO <sub>2</sub> substrate	10 <sup>-5</sup> – 10 <sup>-1</sup>	0.00001	46
AuNPs-polydopamine	ITO	4-800	1.00	18
Graphene oxide nanosheets/polyaniline /CdSe quantum dot	GCE	0.5-10 <sup>4</sup>	0.17	17
3-aminopropyltriethoxy silane (APTES)	Dip-probe	-	0.12	47
p-aminobenzoic acid/p-aminothiophenol/AuNPs	GCE	5-10 <sup>5</sup>	1.60	19
AuNPs	Gold	0.02-20	0.02	48
Polypyrrole-AuNPs	Graphite screen printed electrode (SPE)	1-15x10 <sup>6</sup>	0.33	14
11-mercaptoundecanic acid/6-mercapto-1-hexanol	Gold chip	-	1.30	49
Polydopamine	Glass	2-2000	2.00	50
Europium nanoparticles	LFA	2-500	0.37	51
APTES	Optic fiber	0.4-400	0.10	52
SWCNTs	Graphite SPE	0.5-30	0.50	53
PPyr-NHS Polymer	ITO	0.03-22.5	0.01	This work
ELISA	-	10.24-400	1.00	54

ELISA	-	15.6-10 <sup>3</sup>	5.00	55
ELISA	-	3-1000	3.00	56
ELISA	-	7.81-500	4.69	57

(B)	Found by biosensor (pg/mL)	SD*	Found by biosensor after IL 6 addition (0.5 pg/mL)	SD*	Recovery (%)
1	0.59	0.04 %	1.09	0.02 %	100.18
1	0.54	0.02 %	1.06	0.02 %	100.83
2	0.65	0.02 %	1.12	0.02 %	97.95
2	0.61	0.02 %	1.16	0.02 %	104.0
3	0.71	0.02 %	1.23	0.04 %	101.57
3	0.74	0.02 %	1.17	0.04 %	95.0
4	0.68	0.04 %	1.12	0.05 %	94.78
4	0.63	0.04 %	1.20	0.05 %	105.80
5	0.78	0.03 %	1.24	0.04 %	97.16
5	0.74	0.03 %	1.29	0.04 %	104.64

SD\* : Standard deviation.

## Conclusion

An ultrasensitive label-free electrochemical immunosensor based on *PPyr-NHS* modified ITO electrode was developed for determination of IL 6 antigen. *PPyr-NHS* polymer as an interface material improved the electron transfer efficiency and provided attachment points for IL6R. Furthermore, *PPyr-NHS* polymer was employed as an electrode matrix material for the first time. The basic principle of this analytical tool was based on the covalently immobilization of IL 6R on *PPyr-NHS* modified ITO electrode. During the immobilization, this tool did not require a crosslinking agent. The designed immunosensor offered excellent advantages

like long storage-stability, good selectivity and sensitivity because of the covalently attachment of IL 6R on the sensing surface, and the usage of PPy-NHS polymer increased surface area. The proposed immunosensor could sensitively detect IL 6 antigen in a range from 0.03 pg/mL and 22.5 pg/mL with a detection limit of 10.2 fg/mL. Additionally, it illustrated good repeatability and excellent reproducibility for IL 6 antigen detection. The developed biosensor could be regenerated by immersion in acidic solution, and the regenerated surface could be reused at least 8 times. Moreover, the developed immunosensor had low cost than traditional ELISA kit. In conclusion, the designed immunosensor will not only be proper for determination of IL 6 as shown above but also for other cancer biomarkers.

### Acknowledgements

This research was supported The Scientific and Technological Research Council of by Tekirdağ Namik Kemal University, NKU-BAP (Grant number: NKUBAP.00.ÖNAP.19.209).

### References

- Z. k. Farka, T. s. Juřík, D. Kovář, L. e. Trnková and P. Skládal, *Chemical reviews*, 2017, **117**, 9973-10042.
- J. Guo, C. M. O'Driscoll, J. D. Holmes and K. Rahme, *International journal of pharmaceutics*, 2016, **509**, 16-27.
- X. Chen, Y. Ba, L. Ma, X. Cai, Y. Yin, K. Wang, J. Guo, Y. Zhang, J. Chen and X. Guo, *Cell research*, 2008, **18**, 997-1006.
- C. Kin, E. Kidess, G. A. Poultides, B. C. Visser and S. S. Jeffrey, *Expert review of molecular diagnostics*, 2013, **13**, 581-599.
- J. A. Ludwig and J. N. Weinstein, *Nature Reviews Cancer*, 2005, **5**, 845-856.
- C. Zhou, D. Liu, L. Xu, Q. Li, J. Song, S. Xu, R. Xing and H. Song, *Scientific reports*, 2015, **5**, 9939.
- S. K. Arya and P. Estrela, *Sensors*, 2018, **18**, 2010.
- M. Aydın, E. B. Aydın and M. K. Sezginürk, *Biosensors and Bioelectronics*, 2019, **126**, 230-239.
- M. Aydın, E. B. Aydın and M. K. Sezginürk, *Macromolecular Bioscience*, 2019, **19**, 1900109.
- M. e. T. Castañeda, S. Alegret and A. Merkoci, *Electroanalysis: An International Journal Devoted to Fundamental and Practical Aspects of Electroanalysis*, 2007, **19**, 743-753.
- C. Tian, L. Wang, F. Luan, X. Fu, X. Zhuang and L. Chen, *Chemical Communications*, 2019, **55**, 12479-12482.
- K.-Z. Liang, J.-S. Qi, W.-J. Mu and Z.-X. Liu, *Bioprocess and biosystems engineering*, 2009, **32**, 353-359.
- H. Chen, T. K. Choo, J. Huang, Y. Wang, Y. Liu, M. Platt, A. Palaniappan, B. Liedberg and A. I. Y. Tok, *Materials & Design*, 2016, **90**, 852-857.
- M. Tertiş, B. Ciui, M. Suci, R. Săndulescu and C. Cristea, *Electrochimica Acta*, 2017, **258**, 1208-1218.
- G.-C. Fan, X.-L. Ren, C. Zhu, J.-R. Zhang and J.-J. Zhu, *Biosensors and Bioelectronics*, 2014, **59**, 45-53.
- G. A. Messina, N. V. Panini, N. A. Martinez and J. Raba, *Analytical biochemistry*, 2008, **380**, 262-267.
- P.-Z. Liu, X.-W. Hu, C.-J. Mao, H.-L. Niu, J.-M. Song, B.-K. Jin and S.-Y. Zhang, *Electrochimica Acta*, 2013, **113**, 176-180.
- G. Wang, H. Huang, G. Zhang, X. Zhang, B. Fang and L. Wang, *Langmuir*, 2011, **27**, 1224-1231.
- M. Tertiş, P. I. Leva, D. Bogdan, M. Suci, F. Graur and C. Cristea, *Biosensors and Bioelectronics*, 2019, **137**, 123-132.
- E. O. Blair and D. K. Corrigan, *Biosensors and Bioelectronics*, 2019.
- A. Sassolas, L. J. Blum and B. D. Leca-Bouvier, *Biotechnology advances*, 2012, **30**, 489-511.
- W. Putzbach and N. J. Ronkainen, *Sensors*, 2013, **13**, 4811-4840.
- L. Wu and X. Qu, *Chemical Society Reviews*, 2015, **44**, 2963-2997. DOI: 10.1039/D0NJ03183F
- M. Perfézou, A. Turner and A. Merkoçi, *Chemical Society Reviews*, 2012, **41**, 2606-2622.
- S. Campuzano, M. Pedrero and J. M. Pingarrón, *Sensors*, 2017, **17**, 1993.
- F. Teles and L. Fonseca, *Materials Science and Engineering: C*, 2008, **28**, 1530-1543.
- T. Ahuja and D. Kumar, *Sensors and Actuators B: Chemical*, 2009, **136**, 275-286.
- T. Ahuja, I. A. Mir and D. Kumar, *Biomaterials*, 2007, **28**, 791-805.
- A. Mohamad, M. Rizwan, N. A. Keasberry, A. S. Nguyen, T. Dai Lam and M. U. Ahmed, *Biosensors and Bioelectronics*, 2020, **155**, 112108.
- T.-P. Huynh, P. S. Sharma, M. Sosnowska, F. D'Souza and W. Kutner, *Progress in Polymer Science*, 2015, **47**, 1-25.
- R. Jain, N. Jadon and A. Pawaiya, *TrAC Trends in Analytical Chemistry*, 2017, **97**, 363-373.
- J. Lai, Y. Yi, P. Zhu, J. Shen, K. Wu, L. Zhang and J. Liu, *Journal of Electroanalytical Chemistry*, 2016, **782**, 138-153.
- W. Khan, M. Kapoor and N. Kumar, *Acta Biomaterialia*, 2007, **3**, 541-549.
- B. Neises and W. Steglich, *Angewandte Chemie International Edition in English*, 1978, **17**, 522-524.
- M. Aydın, *Biosensors and Bioelectronics*, 2019, **144**, 111675.
- E. B. Aydın, M. Aydın and M. K. Sezginürk, *Biosensors and Bioelectronics*, 2017, **97**, 169-176.
- S. Bousalem, A. Yassar, T. Basinska, B. Miksa, S. Slomkowski, A. Azioune and M. Chehimi, *Polymers for Advanced Technologies*, 2003, **14**, 820-825.
- H. C. Kim, S. K. Lee, S. W. Lee and S. W. Jeong, *Polymers for Advanced Technologies*, 2009, **20**, 298-302.
- M. Aydın, E. B. Aydın and M. K. Sezginürk, *Biosensors and Bioelectronics*, 2018, **107**, 1-9.
- P. McKittrick and J. Katon, *Applied spectroscopy*, 1990, **44**, 812-817.
- T. Kitagawa and S. Hirota, *Handbook of vibrational spectroscopy*, 2006.
- L. Wang, R. Ma, L. Jiang, L. Jia, W. Jia and H. Wang, *Biosensors and Bioelectronics*, 2017, **92**, 390-395.
- E. B. Aydın, *Talanta*, 2020, 120909.
- S. Zhang, X. Zhuang, D. Chen, F. Luan, T. He, C. Tian and L. Chen, *Microchimica Acta*, 2019, **186**, 450.
- C. Tian, L. Wang, F. Luan and X. Zhuang, *Talanta*, 2019, **191**, 103-108.
- T. Yang, S. Wang, H. Jin, W. Bao, S. Huang and J. Wang, *Sensors and Actuators B: Chemical*, 2013, **178**, 310-315.
- R. Kapoor and C.-W. Wang, *Biosensors and Bioelectronics*, 2009, **24**, 2696-2701.
- L. S. Kumar, X. Wang, J. Hagen, R. Naik, I. Papautsky and J. Heikenfeld, *Analytical Methods*, 2016, **8**, 3440-3444.
- T.-H. Chou, C.-Y. Chuang and C.-M. Wu, *Cytokine*, 2010, **51**, 107-111.
- M. Toma and K. Tawa, *ACS applied materials & interfaces*, 2016, **8**, 22032-22038.
- D. Huang, H. Ying, D. Jiang, F. Liu, Y. Tian, C. Du, L. Zhang and X. Pu, *Analytical biochemistry*, 2020, **588**, 113468.
- K. Zhang, G. Liu and E. M. Goldys, *Biosensors and Bioelectronics*, 2018, **102**, 80-86.
- R. Malhotra, V. Patel, J. P. Vaquero, J. S. Gutkind and J. F. Rusling, *Analytical chemistry*, 2010, **82**, 3118-3123.
- <https://www.thermofisher.com/elisa/product/IL-6-Human-ELISA-Kit/EH2IL6>
- <https://www.mybiosource.com/human-elisa-kits/il-6/355306>
- <https://www.raybiotech.com/human-il6-elisa-kit/>
- [www.elabscience.com/phuman\\_il\\_6\(interleukin\\_6\)\\_elisa\\_kit-17965.html](http://www.elabscience.com/phuman_il_6(interleukin_6)_elisa_kit-17965.html)

View Article Online  
DOI: 10.1039/D0NJ03183F

New Journal of Chemistry Accepted Manuscript

1  
2  
3  
4  
5  
6  
7  
8  
9  
10  
11  
12  
13  
14  
15  
16  
17  
18  
19  
20  
21  
22  
23  
24  
25  
26  
27  
28  
29  
30  
31  
32  
33  
34  
35  
36  
37  
38  
39  
40  
41  
42  
43  
44  
45  
46  
47  
48  
49  
50  
51  
52  
53  
54  
55  
56  
57  
58  
59  
60